https://doi.org/10.5194/egusphere-2026-1811
Preprint. Discussion started: 4 June 2026

Multi-Temporal Influences of Large-Scale Atmospheric Patterns On Antarctic Coastal Polynyas

Jason M. Ward[1] and Marilyn N. Raphael[1]
[1]Department of Geography, University of California, Los Angeles, Los Angeles, CA, 90095, USA
Correspondence to: Jason M. Ward (jward31@ucla.edu)

Abstract. During the austral ice advance season, sea ice expands across the Southern Ocean, significantly reducing gas, heat, and moisture transfer between the atmosphere and ocean. Situated along the Antarctica coastline are areas of open water, minimal sea ice concentration, or relatively thin ice - called coastal polynyas. Coastal polynyas continuously reconnect the atmosphere and ocean. Antarctic coastal polynyas' greatest geographic influence occurs through their contribution to deep water formation and the global Thermohaline Circulation. Coastal polynya impacts are partially controlled by their size. Larger polynyas allow greater rates of sea ice production, bottom water formation, and total biological productivity. This study examines the role that large-scale atmospheric patterns play in Antarctic coastal polynya size variability. The Southern Annular Mode (SAM), El Niño-Southern Oscillation (ENSO), and the Amundsen Sea Low (ASL) together significantly influence the sizes of 20 of the 25 Antarctic coastal polynyas in this study. The SAM exerts its strongest influence in East Antarctica, where a +SAM stunts coastal polynya growth. ENSO, a tropical phenomenon with significant West Antarctica teleconnections, promotes polynya growth during La Niña. The ASL, an exclusively West Antarctica phenomenon, enhances polynya growth in the Amundsen and Bellingshausen Seas as it intensifies and as it migrates northeast. In contrast, an eastward migration of the ASL suppresses polynya expansion in the Weddell Sea. Variability in the SAM and in the ASL's intensity and latitudinal location impact monthly and seasonal polynya size variability. Variability in ENSO and in the ASL's intensity and longitudinal location impact annual, seasonal, and monthly polynya size variability, respectively.

1. Introduction

Every year, during the austral ice advance season, the sea ice field expands to cover on average 19 million km^2 of the Southern Ocean [Maksym et al., 2012]. This sea ice creates a barrier between the ocean and atmosphere, significantly reducing gas, heat, and moisture transfers [Fiedler et al., 2010; Arrigo and van Dijken, 2003]. However, situated around the Antarctic continent, in the pack ice and along the coastal regions, are polynyas, areas of open water or minimal sea ice concentration and thickness surrounded by relatively thick ice [Nihashi et al., 2017; Nihashi and Ohshima, 2015; Comiso et al., 2011; Drucker et al., 2011; Tamura et al., 2008; Martin et al., 2007; Kwok et al., 2007; Arrigo and van Dijken, 2003]. Their formation, decay, and function are products of sea ice production, melt, and transport processes.

https://doi.org/10.5194/egusphere-2026-1811
Preprint. Discussion started: 4 June 2026

Coastal polynyas develop from wind-driven ice divergence away from a static feature such as a coastline, ice tongue, or iceberg. Offshore polynyas are able to balance heat lost to the atmosphere with heat brought to the surface from the subsurface ocean [Goosse and Fichefet, 2001]. However, most coastal polynya heat loss is not replaced from below because the entire water column in shallow shelf regions is near freezing [Nicholls, 2001; Zwally et al., 1985]. The net negative energy imbalance results in a change of state through freezing [Adolphs and Wendler, 1995]. Coastal polynyas are maintained through continuous rates of sea ice export that equal or exceed rates of sea ice production. Static, or slow-moving, features form the windward boundary of these latent heat-induced polynyas. The transported pack ice forms their leeward boundaries [Adolphs and Wendler, 1995; Smith et al., 1990]. Due to the continuous ice advection, coastal polynyas are sites of continued rapid ice production throughout the ice advance season [Ackley et al., 2001; Massom et al., 1998].

Coastal polynyas' greatest geographic influence occurs through deep water formation. Most brine is rejected during the freezing process. Thus, as the surface ocean layer cools, it becomes saltier and denser. Due to continued rapid ice formation within coastal polynyas, surface waters become dense enough to sink to the continental shelf, contribute to high salinity shelf water, and eventually spill into Antarctic Bottom Water [Yang et al., 2025; Mizuta et al., 2024; Fiedler et al., 2010; Ushio et al. 1999; Smith et al., 1990]. Antarctic Bottom Water feeds into the Thermohaline Circulation, also known as the Meridional Overturning Circulation, which gives Antarctic coastal polynyas global influence. Deep ocean processes like the Thermohaline Circulation occur on the order of centuries and provide important long-term storage for greenhouse gases, such as carbon dioxide [Kitade et al., 2014; Shadwick et al., 2013; Beckmann et al., 1999]. The impacts that coastal polynyas have on the ocean's thermodynamic, chemical, biological, and gas processes are controlled by polynya size. Larger polynyas allow greater rates of sea ice production, bottom water formation, and total biological productivity [Yang et al., 2025; Tamura et al., 2016]. Thus, it is useful to understand the influences impacting changes in coastal polynya size.

Variability in coastal polynya size is linked to wind-driven sea ice advection created by katabatic winds and thermodynamic processes that determine ice production rates [Holland and Kwok, 2012]. Surface winds may be enhanced or dampened by the Southern Ocean sea level pressure field which is connected to large-scale atmospheric patterns [Turner et al., 2016]. This paper examines the role that the large-scale atmospheric patterns play in Antarctic coastal polynya size variability.

Coastal polynyas generate 5-10% of Weddell Sea ice, 20-50% of Ross Sea ice, and 10% of total Antarctic sea ice [Tamura et al., 2008; Kwok et al., 2007]. With much of the Southern Ocean sea ice content originating at the coast, variability in coastal polynya activity has the potential to influence significant changes in the sea ice field. Furthermore, the interaction between large-scale atmospheric phenomena and the sea ice field is potentially influenced by intermediary mechanisms that include coastal polynyas.

Current coastal polynya literature lacks deep investigation into the relationships between Antarctic coastal polynya size variability and large-scale atmospheric circulation patterns. However, there are a few studies that suggest an influence. Arrigo and van Dijken [2003], using a six-year dataset, pointed out that years of anomalously low Ross Sea Polynya area appeared concurrent with a strong positive El Niño-Southern Oscillation (ENSO) event.

https://doi.org/10.5194/egusphere-2026-1811
Preprint. Discussion started: 4 June 2026

Montes-Hugo and Yuan [2012] found that the size of the phytoplankton bloom in the post-polynya region of Dumont d'Urville was positively related to the Southern Annular Mode (SAM). It is important to note that phytoplankton bloom production is most active during spring and summer, which creates a temporal disconnect between the phytoplankton blooms and wintertime polynyas.

Using four years of automatic weather station data, Bromwich et al. [1998] linked ENSO to polynya-producing katabatic surge events in the coastal Ross Sea. Park et al. [2018] compares nonlinear trends in the Ross Ice Shelf Polynya's (RISP) activity to the SAM and ENSO. They found that trends in RISP area and timing of the RISP's annual occurrence are influenced by trends in ENSO and the SAM, respectively. Tamura et al. [2016] correlated the SAM and ENSO indices with circumpolar Antarctic coastal polynyas but found generally weak correlations with both. As discussed below, our study found strong influences from the SAM and ENSO on coastal polynya size variability around the continent.

Studies have identified a significant connection between the presence of polynyas near the Maud Rise region and a negative SAM phase (-SAM). The upward transport of oceanic heat, which is associated with the basal sea ice melt that opens the offshore polynyas, is prompted by the descent of relatively high salinity surface water [Silvano et al., 2025]. This vertical instability is associated with -SAM conditions. In contrast, persistent reduction in surface salinity, such as during a positive SAM phase (+SAM), reduces upward transport of the relatively warm water from below, the associated basal sea ice melt, and subsequent formation of the offshore polynyas [Cheon and Gordon, 2019; Campbell et al., 2019]. Since these sensible heat-induced polynyas are associated with offshore sea ice melt, they are not associated with ice production, which is promoted by wind-driven conditions at the coast. Jiang et al. [2024] found a similar connection between a +SAM and enhanced chlorophyll concentration within the Marguerite Bay Polynya, situated along the western coast of the Antarctic Peninsula. This relationship is not directly associated with polynya size because it focuses on chlorophyll concentration, rather than total chlorophyll.

Not only are studies on coastal polynya responses to large-scale atmospheric activity scarce, but they are generally limited to a few large and prominent polynyas – e.g., polynyas in the Ross, Weddell, and Amundsen Seas [Park et al., 2018; Tamura et al., 2016; Arrigo and van Dijken, 2003; Bromwich et al., 1998]. Also, studies are often done at annual or three-month seasonal average time scales and thus are too broad to capture much of the co-variability at finer timescales.

The link between large-scale atmospheric circulation patterns and Antarctic coastal polynyas arises from the atmospheric patterns' influence on surface winds and the sea ice field. However, the connection is often complicated by coastal geometry, which influences direction of growth [Nihashi and Ohshima, 2015; Shadwick et al., 2013; Massom et al., 1998]. Here, we use a 26-year monthly polynya area dataset [Ward & Raphael, 2018] to investigate the response of individual Antarctic coastal polynyas to large-scale atmospheric patterns, including the SAM, ENSO, and the Amundsen Sea Low (ASL) (Fig. 1). We also provide brief commentary on the impact of local coastal geometry on coastal polynya relationships with large-scale atmospheric phenomena. Section 2 of this paper describes the datasets and methods used in the study. Section 3 presents the results. Section 4 provides a discussion and summary.

https://doi.org/10.5194/egusphere-2026-1811
Preprint. Discussion started: 4 June 2026

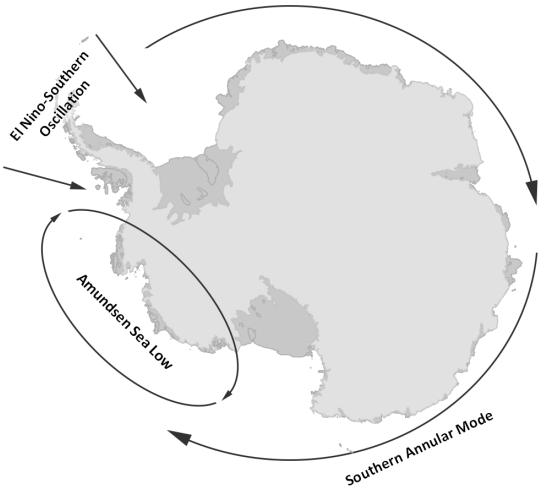

Figure 1: The scale, direction of motion, and distribution of three prominent atmospheric phenomena: the Southern Annular Mode (SAM), El Niño-Southern Oscillation (ENSO), and the Amundsen Sea Low (ASL). The SAM circles Antarctica. ENSO and the ASL influence West Antarctica.

2. Data and Methodology

2.1 Coastal Polynya Data

This study utilizes an Antarctic coastal polynya area dataset that ranges from 1992-2017 during the April-October polynya season. The dataset was processed from daily coastal polynya area estimates. The daily estimates were extracted using thin ice and fast ice detection methodologies [Tamura et al., 2007] applied to satellite imagery inputs from the Defense Meteorological Satellite Program's Special Sensor Microwave Imager (SSM/I) series brightness temperature data. SSM/I series data is distributed by the National Snow and Ice Data Center (NSIDC) in the 'DMSP SSM/I-SSMIS Pathfinder Daily EASE-Grid Brightness Temperatures, Version 2' dataset [Armstrong et al., 1994]. The 25-polynya dataset is accessible through the Github data repository: Ward & Raphael [2018] - ACP25 (https://github.com/JWard31/atmos_poly/blob/e325cc43753bc6f2129a79bda6b575348879f7b5/Ward%20and%20Raphael%20-%20ACP25%20-%2025%20Antarctic%20Coastal%20Polynyas%201992-2017.csv). Ward [2018] provides a detailed application of the polynya detection algorithms used to create the dataset. While 70 polynyas were identified, the dataset employed in this study focuses on the 25 polynyas with a minimum mean surface area of 1,562.5 km^2 - the size of 10 12.5x12.5 km pixels - to capture non-negligible variability and at least 30% daily occurrence - defined as a surface area greater than 0 km^2 (Fig. 2a). Tamura et al. [2007] identified 13 Antarctic coastal polynyas as the largest contributors to Antarctic polynya sea ice production. All 13 are included in the 25-polynya dataset employed in the current study. Therefore, the vast majority of coastal polynya ice production occurs in the largest 25 polynyas used here.

https://doi.org/10.5194/egusphere-2026-1811
Preprint. Discussion started: 4 June 2026

Each daily coastal polynya time series was initially aggregated to annual means to highlight their long-term tendencies. Linear trendlines were calculated from the initial annual means and regressed against the original daily data series. Standardized deviations from the trendlines were aggregated to the monthly means that are utilized in this study. This process is performed to eliminate the over-allocation of atmosphere-polynya correlation due to long term trends.

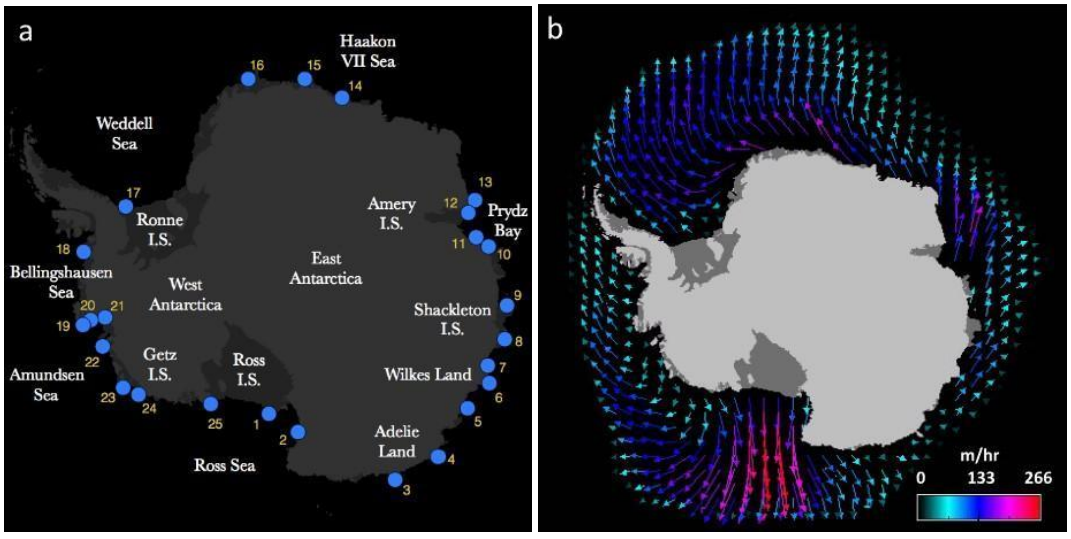

Figure 2: a) Locations of the largest 25 Antarctic coastal polynyas. Relevant oceanic and continental place names are labeled. Light and dark grey areas represent landmasses and ice shelves, respectively. b) Mean direction and magnitude of sea ice motion during the polynya season (April-October) from 1992-2017. The color of the arrows indicate speed of motion with units in meters per hour.

1. Ross Ice Shelf (RIS)
2. Terra Nova Bay (TNB)
3. Mertz Glacier (MG)
4. Dibble Glacier (DG)
5. Dalton (Da)
6. Cape Poinsett (CP)
7. Vincennes Bay (VB)
8. Shackleton Ice Shelf (SIS)
9. Davis Sea (DS)
10. Barrier Bay (BaB)
11. Prydz Bay (PB)
12. Mackenzie Bay (MB)
13. Cape Darnley (CD)
14. Breid Bay (BrB)
15. East Lazarev Ice Shelf (ELIS)
16. Jelbart Ice Shelf (JIS)
17. Ronne Ice shelf (RON)
18. Bellingshausen Sea (BS)
19. Ferrero Bay (FB)
20. Cranton Bay (CB)
21. Pine Island Bay (PIB)
22. Amundsen Sea (AS)
23. Wrigley Gulf (WG)
24. Getz Ice Shelf (GIS)
25. Okuma Bay (OB)

https://doi.org/10.5194/egusphere-2026-1811
Preprint. Discussion started: 4 June 2026

Figure 2b displays mean sea ice motion (i.e., direction and velocity) during the polynya season from 1992-2016. At the time of the dataset creation, sea ice motion data availability only extended to February, 2017. The ice motion data are distributed by the National Snow and Ice Data Center (NSIDC) in the "Polar Pathfinder Daily 25 km EASE-Grid Sea Ice Motion Vectors, Version 3" dataset [Tschudi et al., 2016]. The greatest Southern Ocean ice velocity occurs as southerly flow through the Ross Sea, after divergence from the Ross Ice Shelf. After ice exits the Ross Sea embayment, it veers westerly and flows through the Ross Gyre. Weddell Sea ice motion flows in a clockwise motion through the Weddell Gyre. East Antarctica sea ice motion is characterized by easterly flow within its relatively short pack ice extent.

2.2 Atmospheric Data

Monthly mean indices that describe the Southern Annular Mode (SAM), El Niño-Southern Oscillation (ENSO), and the Amundsen Sea Low (ASL) were retrieved from multiple sources as subsets during the polynya season (April-October) from 1992 to 2017. The SAM index, described by Marshall [2003], is housed at the British Antarctic Survey [BAS; https://legacy.bas.ac.uk/met/gjma/sam.html]. A positive SAM index represents an increase in the meridional pressure gradient and the corresponding intensification of circumpolar westerly winds. The Southern Oscillation Index (SOI) used to quantify the sign and strength of ENSO is described and distributed by the National Oceanic and Atmospheric Administration [https://www.cpc.ncep.noaa.gov/data/indices/soi]. Relatively strong positive SOI anomalies are associated with the ENSO warm phase (El Niño). Relatively strong negative SOI anomalies are associated with the ENSO cool phase (La Niña). The ASL dataset is also distributed by BAS, and it was created using the method described by Hosking et al. [2013; https://scotthosking.com/asl_index]. Four indices, which together completely characterize the ASL, are provided – actual central pressure (ACP), relative central pressure (RCP), longitude (LON), and latitude (LAT).

To analyze the influence of large-scale atmospheric patterns on Antarctic coastal polynya size variability and determine the temporal scales at which these relationships take place, the general trend of all polynya and atmospheric data series were removed and the annual, seasonal, and monthly variability of the atmospheric data series were isolated into distinct components. This was completed using a time series decomposition method that successively applies multiplicative linear regression to the temporal components of each atmospheric index [Faraway, 2014].

Since the atmospheric data are provided as monthly means, each monthly atmospheric index was initially aggregated to annual means to highlight their long-term tendencies. Linear trendlines were calculated from the initial annual means and regressed against the original monthly timeseries. Standardized deviations from the trendlines were aggregated to monthly climatologies - hereafter referred to as seasonal variability. Standardized deviations from the seasonal variability were aggregated to annual means, and their standardized deviations represent the monthly variability utilized in this study. This stepwise regression process distinguishes uncorrelated

https://doi.org/10.5194/egusphere-2026-1811
Preprint. Discussion started: 4 June 2026

temporal scales of variability - the trend, seasonal, annual, and monthly components are mutually exclusive (R^2=0) - and accounts for all of the variability within the original, complete data sets (R^2=1). Thus, each temporal component uniquely contributes to the total variability, which is important for identifying influential scales of variability. Figure 3 shows the percent contribution of each atmospheric pattern's temporal components to its total pattern variability.

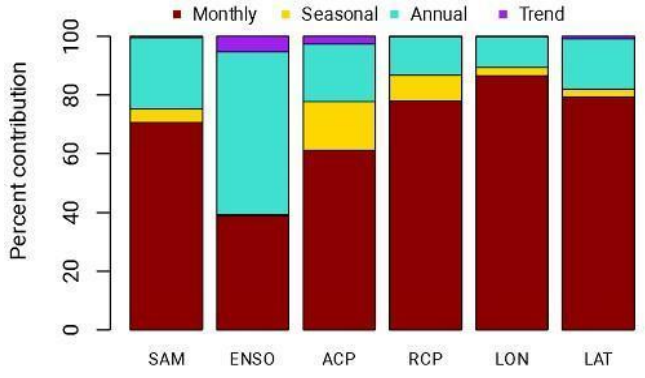

Figure 3: Relative contributions of each temporal component (linear trend and exclusive monthly, seasonal, and annual variability) to the total variability of large-scale atmospheric patterns.

The SAM index has a relatively weak positive trend that accounts for 0.6% of the total variability in the study period (Fig. 3). Its exclusive annual, seasonal, and monthly variability account for approximately 24%, 4.5%, and 71% of its total variability, respectively. The SAM's seasonality has its winter minimum (maximum) in June (August) (not shown). While ENSO (measured by the SOI) had a general decline through the latter half of the 20th century [Nicholls, 2008], it exhibited a relatively strong positive trend during the study period, which accounts for 5.4% of its total variability. It exhibits minimal seasonality with annual and monthly variability accounting for approximately 55.4% and 39% of its total, respectively.

Decomposition of the ASL's actual central pressure index (ACP) reveals a negative trend, accounting for approximately 2.6% of its variability. Exclusive annual, seasonal, and monthly scale variability account for approximately 20%, 16.6%, and 61% of its total, respectively. The ASL's location (i.e., LON, LAT) is highly variable with exclusive annual, seasonal, and monthly variability accounting for approximately 10.5%, 3%, and 86.6% of total LON variability, respectively, and 17%, 3%, and 79% of total LAT variability, respectively.

The ASL's central location experienced a southeastward trend over the study period. While the southward trend over time agrees with Turner et al. [2013], the eastward trend in the current study opposes the westward trend found in theirs. The difference is due to the different study periods, with theirs ranging between 1979-2008 and the current study ranging between 1992-2017. Studies have found positive relationships between ENSO and LON, with El Niño promoting an eastward shift in the ASL's longitude [Turner et al., 2013; Yuan, 2004]. A statistically significant

https://doi.org/10.5194/egusphere-2026-1811
Preprint. Discussion started: 4 June 2026

positive relationship between ENSO and ASL's longitude is discussed later in this paper (Fig. 8). With the positive long term trend previously presented in this paper (Fig. 3), ENSO has a greater tendency towards El Niño conditions throughout the study period, which promotes the eastward ASL migration reported. However, the long term trends found in the current study account for less than 1% of the location variability in both directions.

Seasonally, LON and LAT have concurrent extremes with northern and western maxima in June and southern and eastern maxima in August. The seasonal variability of all ASL metrics are consistent with those found by Hosking et al. [2013] and Turner et al. [2013], except their northern LAT maximum occurs in May. The temporal range covered by Hosking et al. [2013] is different from that covered by the current study, which may contribute to the slight discrepancy.

2.3 Polynya-Atmosphere Regression

This study quantifies the partial contribution of each atmospheric pattern's annual, seasonal, and exclusive monthly variability to the variations in Antarctic coastal polynyas' sizes. To do so, multivariate regression analysis was performed. Each polynya's detrended time series was regressed against each atmospheric pattern's exclusive annual, seasonal, and monthly components (Eq. 1), identified by the stepwise decomposition described above. Each multivariate regression model's coefficient of determination (R^2) is employed to measure the influence of the atmospheric pattern's temporal components on polynya size variability. The relative contribution of each temporal component is calculated as the relative contribution of their individual t-values (provided in the regression model's output) to the total sum of t-values in the model. All statistically significant relationships are determined at the 90% significance level. In Eq. 1, $Polynya_{Total}$ is the inclusive monthly polynya variability (with annual and seasonal variability included) and $Atmos_{Monthly}$ is an atmospheric pattern's exclusive monthly variability (with annual and seasonal variability removed).

$$Polynya_{Total} \sim Atmos_{Annual} + Atmos_{Seasonal} + Atmos_{Monthly} \quad (1)$$

3. Results

As stated above, coastal polynyas develop from wind-driven ice advection from the coast, and other virtually static features, as sea ice is continuously generated through heat lost to the atmosphere. Stronger surface winds flowing away from the virtually static features increase coastal polynya size. Weaker surface winds flowing in the same direction, or a reversal in wind direction, decrease coastal polynya size. Similar changes in ocean and sea ice motion have similar effects on coastal polynya size. Thus, processes that impact the strength and direction of surface winds along the coast, such as the large-scale atmospheric patterns discussed here, affect polynya size variability.

https://doi.org/10.5194/egusphere-2026-1811
Preprint. Discussion started: 4 June 2026

3.1 Southern Annular Mode

Relationships between coastal polynyas and the SAM are particularly strong in East Antarctica from Adelie Land to Prydz Bay (Fig. 4). This is consistent with the finding that, with respect to its impact on sea ice variability, the SAM is the dominant large-scale atmospheric circulation pattern in that region. Eight of the eleven polynyas have statistically significant negative relationships suggesting that under +SAM conditions they shrink in size. The strong polynya relationships in that region are primarily driven by seasonal and monthly scale co-variability. The Haakon VII Sea and West Antarctica regions contain only two strong SAM-polynya relationships. Their co-variability is primarily driven at the monthly scale as well. In regions where coastal polynyas form along ice tongues and other meridionally oriented ice features, anomalous zonal ice flow may have a larger effect on polynya size than meridional anomalies. The increased westerly wind associated with +SAM contributes to westerly sea ice flow anomalies. Thus, polynyas that grow with easterly winds, such as most East Antarctica polynyas [Nihashi and Ohshima, 2015], will decrease with the enhanced westerly winds of +SAM and increase with the weakened westerly winds of -SAM.

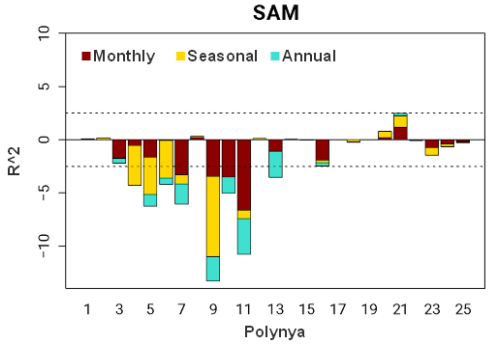

Figure 4: Coefficient of determination (R^2) of multivariate regression model results for each of the 25 Antarctic coastal polynyas regressed against the Southern Annular Mode (SAM). Red, gold, and turquoise represent relative contributions at the exclusive monthly, seasonal, and annual scales of variability, respectively. Dashed lines indicate statistical significance at the 90% level. The data ranges from April-October, 1992-2017.

East Antarctica polynyas, particularly between Adelie Land and Prydz Bay, generally form along the western edge of meridionally oriented features and, thus, grow westward toward more marginal ice areas. Two polynyas within this region are not strongly influenced by the SAM. The first of the two, the Shackleton Ice Shelf Polynya (#8), forms within a small bay of the Shackleton Ice Shelf and does not experience much zonal expansion. The second of the two, the MacKenzie Bay Polynya (#12), forms along the eastern edge of a fast ice feature, which prevents growth westward and allows growth eastward. However, its direction of growth is in competition with the direction of mean ice flow (Fig. 2b), which limits the polynya's eastward expansion as well. This supports the negative relationships found in the nine statistically significant East Antarctica correlations.

Tamura et al. [2016] generally found negative relationships, except in three polynyas (one polynya along each of the Ross, Weddell, and Adelie Land coasts) but report no statistically significant relationships between SAM and the thirteen Antarctic coastal polynyas they studied. However, their analysis used annual cumulative sea ice, instead of monthly polynya size as is done in the current study. To compare our analysis with theirs we calculated the correlation between the polynyas and the SAM index at the annual timescale. As with the Tamura et al. [2016] study,

https://doi.org/10.5194/egusphere-2026-1811
Preprint. Discussion started: 4 June 2026

no statistically significant relationships were found. This highlights the importance of examining these relationships at different timescales of variability. In our analysis we find that most of the strong SAM-polynya relationships are driven by seasonal and monthly variability, both of which are lost in the annual means and cumulative totals that are popularly presented in other studies. We note also that monthly variability contributes the most to the total variability of the SAM (Fig. 3).

Studies have revealed a late 20th/early 21st century tendency towards a more +SAM [Cheon and Gordon, 2019; Thompson et al., 2011; Gillett et al., 2008; Turner et al., 2009; Arblaster and Meehl, 2006; Marshall, 2003]. The Cape Darnley Polynya (#13) has a statistically significant negative trend in size, as well as a strong negative trend in ice production [Tamura et al., 2016; Nihashi and Ohshima, 2015]. We found that its size variability has a statistically significant negative relationship with the SAM. Thus, the long-term reduction in the Cape Darnley Polynya area may support a possible connection to the long-term positive linear trend of the SAM.

3.2 El Niño-Southern Oscillation

The relationships between coastal polynyas and ENSO are particularly strong in the Amundsen Sea where three of the five polynyas (#19, 20, and 23) have statistically significant positive relationships (Fig. 5). This is the region whose sea ice variability is most strongly affected by ENSO [e.g. Raphael and Hobbs, 2014; Stammerjohn et al., 2008]. During La Niña events, when the Southern Oscillation Index (SOI) is anomalously positive, the subtropical jet weakens and the polar frontal jet strengthens, directing more storms to the west of the Antarctic Peninsula. This establishes a low pressure center in the Amundsen and Bellingshausen region, which directs southerly winds away from the coast and promotes polynya expansion in the Amundsen Sea. During El Niño events, when the SOI is anomalously negative, more storm activity occurs east of the peninsula and a relatively high pressure center is established in the Amundsen and Bellingshausen region [Montes-Hugo and Yuan, 2012; Knuth and Cassano, 2011; Yuan, 2004; Yuan and Martinson, 2001], directing northerly winds toward the coast and limiting polynya growth in the Amundsen Sea.

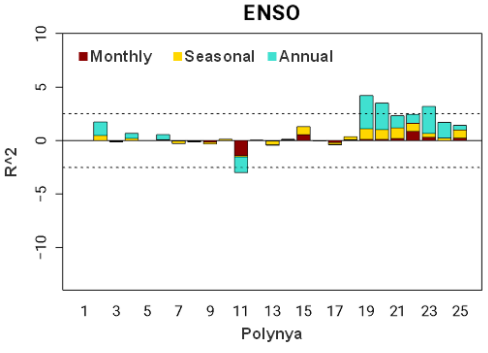

Figure 5: Coefficient of determination (R^2) of multivariate regression model results for each of the 25 Antarctic coastal polynyas regressed against the El Niño Southern Oscillation (ENSO). Red, gold, and turquoise represent relative contributions at the exclusive monthly, seasonal, and annual scales of variability, respectively. Dashed lines indicate statistical significance at the 90% level. The data ranges from April-October, 1992-2017.

ENSO's impact on coastal polynyas is also moderated by its influence on the Amundsen Sea Low (ASL). Due to its impact on the pressure field west of the Antarctic Peninsula (Fig. 1), ENSO has statistically significant relationships

https://doi.org/10.5194/egusphere-2026-1811
Preprint. Discussion started: 4 June 2026

with the ASL's intensity and location. La Niña promotes a stronger ASL - identified by lower actual central pressure (ACP; Fig. 8). As discussed later in this paper, a relatively low ACP is also associated with larger polynyas in the Amundsen and Ross regions (Fig. 6). During La Niña, the center of the ASL tends to be in the Amundsen Sea, while during El Niño it sits in the Ross Sea [Yuan, 2004]. This produces a statistically significant positive correlation between ENSO and the ASL's longitudinal position (LON; Fig. 8). As also discussed later in this paper, an eastern ASL location is associated with larger Amundsen and Bellingshausen coastal polynyas (Fig. 9). Thus, the ENSO-ASL-polynya interaction may confound the significant ENSO-polynya relationships. However, we found that the ENSO-polynya relationships are driven by annual variations, while the ASL's ACP-polynya relationships are driven by monthly and seasonal variations (Fig. 6). Utilization of the multi-temporal analysis in this study allows distinction between coastal polynya responses to ENSO and the ASL.

Tamura et al. (2016) report a statistically significant positive relationship between ENSO and the Amundsen Sea Polynya's (#22 on Fig. 2a) sea ice production. Since they also report a statistically significant positive correlation (r=0.82) between the polynya's ice production and size, their results suggest a strong positive correlation between ENSO and Amundsen Sea Polynya area as well. In our study, the ENSO-polynya area relationship narrowly failed to reach the threshold significance level. However, three of the remaining four polynyas in the Amundsen Sea have statistically significant correlations with ENSO (Fig. 5). Tamura et al. [2016] also reports a statistically significant negative correlation between ENSO and the Cape Darnley Polynya's (#13 on Fig. 2a) sea ice production. We found a weak ENSO relationship with that polynya's size. However, we found a statistically significant negative relationship with the nearby Prydz Bay Polynya (#11 on Fig. 2a).

We did not find statistically significant correlations between ENSO and the Ross Ice Shelf Polynya (#1 on Fig. 2a). However, other studies suggest a connection between ENSO and the overall Ross Sea coastal region. Park et al. [2018] found that the long-term nonlinear trend in the RISP's size is driven by the nonlinear trend in ENSO. Also, Arrigo and van Dijken [2004] report a statistically significant negative annual relationship between ENSO and the Ross Sea post-polynya. They correlate a multivariate ENSO index with total open water area within the entire Ross Sea embayment. While their post-polynya analysis focused on accumulated springtime features, instead of the smaller individual winter features we studied, their results support a connection between ENSO and the Ross Ice Shelf coastal region.

3.3 Amundsen Sea Low: Actual Central Pressure

The Amundsen Sea Low's intensity, measured through its actual central pressure (ACP), is the minimum pressure within the ASL domain. Its central location ranges from 170-290°E longitude and 60-75°S latitude [Hosking et al., 2013]. Relationships between coastal polynyas and ACP are particularly strong in the Amundsen and Ross Seas (Fig. 6). Seven of the nine polynyas in the region have statistically significant negative relationships that are primarily driven by variability at the monthly and seasonal scales. Two polynyas outside of the Ross-Amundsen region have statistically significant positive relationships.

https://doi.org/10.5194/egusphere-2026-1811
Preprint. Discussion started: 4 June 2026

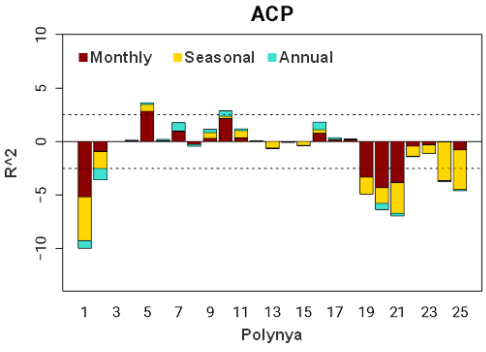

Figure 6: Coefficient of determination (R^2) of multivariate regression model results for each of the 25 Antarctic coastal polynyas regressed against the Amundsen Sea Low's actual central pressure (ACP). Red, gold, and turquoise represent relative contributions at the exclusive monthly, seasonal, and annual scales of variability, respectively. Dashed lines indicate statistical significance at the 90% level. The data ranges from April-October, 1992-2017.

Because the ASL's domain is constrained to West Antarctica (Fig. 1), changes in its intensity are important for West Antarctic climate variability. With its average central location in the Amundsen Sea, its southerly airflow promotes greater Ross and Amundsen Sea ice extent to the west and its northerly airflow promotes smaller Bellingshausen Sea ice extent to the east [Turner et al., 2013; Fogt et al., 2012; Turner et al., 2009]. Thus, the strength of the ASL is expected to influence polynyas differently on either side of its mean central location. Raphael et al. [2019] reports that anomalously intense ASL (identified by a large negative ACP anomaly) is associated with increased northerly surface wind anomalies in the Bellingshausen region and southerly surface wind anomalies in the Ross-Amundsen region. The ASL's effect on meridional surface wind speed allows it to enhance coastal polynya expansion in the Ross and Amundsen Seas and suppress polynya expansion in the Bellingshausen Sea (Fig. 6).

However, our results show no relationship between the Bellingshausen Sea Polynya (#18, Fig. 2a) and ASL's ACP. This may be due to confounding influences from the SAM and ENSO on the ASL and polynyas. When the influence of other large-scale atmospheric phenomena, such as the SAM and ENSO, are removed from the ACP, the ASL's strong influence on the Bellingshausen Polynya's size is identified. This is shown in the Bellingshausen Polynya's relationship with the ASL's relative central pressure (RCP; Fig. 7), which is discussed later in this paper.

Periods of anomalously intense ASL are also associated with negative westerly surface wind anomalies along the west Bellingshausen and Amundsen Sea coasts [Raphael et al., 2019]. With a northwest direction of maximum expansion for the largest polynyas in that region [Nihashi and Ohshima, 2015], the easterly sea ice flow from the Ross Gyre (Fig. 2b) promotes polynya growth. This also supports the negative ACP-polynya relationship, in which an anomalously negative ACP (i.e an intense ASL) is associated with enhanced easterly ice flow and coastal polynya growth.

3.4 Amundsen Sea Low: Relative Central Pressure

The Amundsen Sea Low's relative central pressure (RCP) represents the regional effect of the ASL, with the large-scale background influences removed. In contrast, the ACP is highly influenced by other large-scale processes that impact conditions inside and beyond the ASL domain, such as the SAM, ENSO, and the Semi-Annual

https://doi.org/10.5194/egusphere-2026-1811
Preprint. Discussion started: 4 June 2026

Oscillation [Coggins and McDonald, 2015; Fig. 8 of the current study]. RCP is computed as the difference between the ACP and the actual sector pressure (ASP), which is the mean sea level pressure within the ASL domain [Hosking et al., 2013]. Raphael et al. [2019] showed that the RCP is affected by a pressure ridge north of the ASL domain, indicating the RCP is not completely decoupled from large-scale systems beyond the ASL domain. During the study period, the RCP has a significant positive correlation with ACP (r=0.46; Fig. 8) and is uncorrelated with ASP (r=0.00; not shown). ACP and ASP are highly correlated (r=0.88; not shown) because a decrease in sector pressure includes a decrease in the ASL's central pressure.

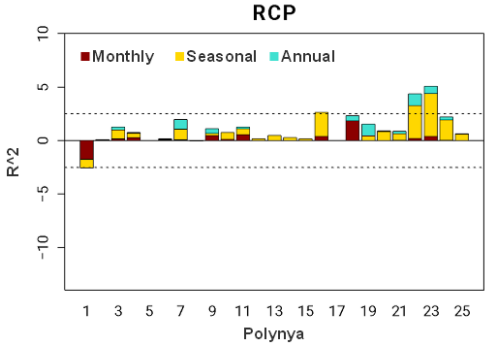

Figure 7: Coefficient of determination (R^2) of multivariate regression model results for each of the 25 Antarctic coastal polynyas regressed against the Amundsen Sea Low's relative central pressure (RCP). Red, gold, and turquoise represent relative contributions at the exclusive monthly, seasonal, and annual scales of variability, respectively. Dashed lines indicate statistical significance at the 90% level. The data ranges from April-October, 1992-2017.

Since the ASL is defined as the lowest pressure center within the ASL domain, its central pressure (ACP) is always lower than the mean background pressure (ASP) throughout the domain. During the study period, the ACP exhibited greater variability than the ASP. When the ASL intensifies, the difference between its central pressure and the background pressure becomes more negative, marking the RCP's identification of an intense ASL anomaly. Thus, an anomalously intense ASL is associated with a decrease in sector pressure (ASP), a larger decrease in ASL central pressure (ACP), an increase in the ACP-ASP difference (in the negative direction), and an anomalously low RCP. A reduction in the ACP that is associated with the ASP (r=0.88, not shown) does not automatically correspond to a strengthening of the ASL's RCP (r=0.46, Fig. 8). Thus, most of the ACP variability is not attributed to the ASL. Since the RCP is an indicator of ASL strength separate from the influence of other nearby phenomena, it is a good metric to utilize for analyses attempting to isolate the impacts of various environmental drivers within the ASL domain.

https://doi.org/10.5194/egusphere-2026-1811
Preprint. Discussion started: 4 June 2026

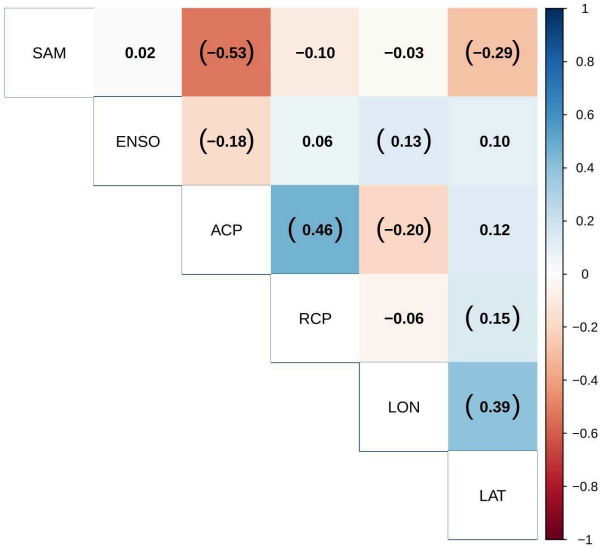

Figure 8: Correlation (r) matrix of large-scale atmospheric pattern variability, including the Southern Annular Mode (SAM), El Nino-Southern Oscillation (ENSO), and the Amundsen Sea Low's actual central pressure (ACP), relative central pressure, longitude (LON), and latitude (LAT). The scale bar indicates the coefficient of correlation (r). Values within parentheses are statistically significant at the 90% significance level.

RCP-polynya relationships are statistically significant in the Amundsen and Ross Seas and are driven by seasonal and monthly co-variability, respectively. Generally, RCP-polynya relationships are positive in the Amundsen-Bellingshausen region (#18-24 Fig. 2a) with strong correlations along the northward-facing coastline (#18, 22-24 Fig. 2a; Fig. 7) and statistically significant correlations in the central Amundsen Sea coastal region (#22-23 Fig. 2a; Fig. 7). Those polynyas are east of the ASL's mean central location (224°E, 70°S) and, thus, are in the region influenced by the northerly and easterly winds of the ASL. A strong ASL is characterized by anomalously negative RCP, relatively strong northerly surface wind in the Amundsen-Bellingshausen coastal region, and strong easterly surface wind along the Amundsen Sea coast [Raphael et al., 2019]. These reduce the strength of the southerly katabatic flow away from the continent, and therefore polynya size. The rigid westward-facing Amundsen Sea embayment's coastline suppresses southerly growth of coastal polynyas but allows their easterly expansion (#19-21 Fig. 2a). It reduces the ASL's effect (as expressed through RCP) on southerly surface wind in that location. In the Ross Sea, the statistically significant RCP-polynya relationship (#1 Fig. 2a; Fig. 7) is negative because of the ASL's impact on southerly surface wind. An anomalously strong ASL is associated with southerly Ross Sea wind anomalies [Raphael et al., 2019] that push coastal sea ice northward and expand the Ross Ice Shelf Polynya.

The RCP and ACP indices present generally opposing polynya statistical relationships within the Amundsen and Ross Seas. Significant positive RCP-polynya relationships correspond to non-significant negative ACP-polynya relationships (#22-23 Fig. 2a). Non-significant positive RCP-polynya relationships correspond to significant negative ACP-polynya relationships (#19-21, #24-25, and #2). Only the Ross Ice Shelf Polynya (#1) deviates from

https://doi.org/10.5194/egusphere-2026-1811
Preprint. Discussion started: 4 June 2026

this pattern (Figs. 5-6). While the ACP and RCP indices are significantly correlated (r=0.46), the majority of ACP's variability is linked to the other large-scale atmospheric phenomena included in this study: SAM and ENSO [Coggins and McDonald, 2015; Fig. 8 of the current study]. The ACP is a compilation of the RCP, SAM, ENSO, and other smaller phenomena (Eq. 2). Thus, removing the influence of the SAM and ENSO from ASL's ACP variability would likely produce a higher correlation with RCP than that found in the current ACP-RCP relationship. In fact, functionally removing the SAM and ENSO is part of the process that creates the RCP index.

$$\text{ACP} = \text{RCP} + \text{SAM} + \text{ENSO} + \text{additional phenomena} \quad (2)$$

There are significant ACP-polynya correlations around Antarctica, even outside of the ASL's domain. This is possible because the strong ACP-polynya correlations are partially a function of ENSO and the SAM's influence on ACP and the polynyas. Since ENSO and the SAM's influences on coastal polynyas are dominant in West and East Antarctica, respectively, their confounding impacts on the ACP-polynya relationships occur in corresponding regions. For instance, an anomalously positive ENSO is associated with larger West Antarctica polynyas (#19-25 in Fig. 5) and a weaker ACP (Fig. 8). Thus, due to the influence of ENSO, larger polynyas and a weaker ACP occur simultaneously (Fig. 6). Likewise, an anomalously positive SAM is associated with smaller East Antarctica polynyas (#3-16 in Fig. 4) and a weaker ACP (Fig. 8). Thus, due to the influence of the SAM, smaller polynyas and a weaker ACP occur simultaneously (Fig. 6). This accounts for the statistically significant positive East Antarctica ACP-polynya correlations, which would not exist without the SAM because they are beyond the ASL's domain of influence. Thus, removing the influence of the SAM and ENSO from the ASL's ACP will result in an index that more closely mimics the RCP and have polynya correlations that more closely resemble the RCP-polynya correlations, which are positive in West Antarctica and not statistically significant in East Antarctica (Fig. 7).

The Ross Ice Shelf Polynya (RISP; #1 in Fig. 2a) is not influenced by the SAM nor ENSO. Therefore, the removal of the SAM and ENSO's influences from the ACP would not impact the ASL-RISP relationship. That is why the ASL-RISP relationship is statistically significant and negative for both the ACP and RCP. Thus, the difference between the ACP and RCP is not their physical functions, but rather, the difference is a result of statistical cleaning of the ACP, which produces the RCP metric. A similar relationship is discussed for the influence of ASL's latitudinal location on East Antarctica coastal polynya size variability later in this paper.

3.5 Amundsen Sea Low: Longitude

The influence of ASL intensity (ACP and RCP) on surface conditions is complicated by the fact that the location of the ASL is variable. Its central position ranges between 170-290°E longitude [Hosking et al., 2013]. During the cold season, the ASL location (LON and LAT) controls the spatial variability of its influence [Coggins and McDonald, 2015]. Thus, understanding the relationship between ASL location and coastal polynya variability is important for a fuller understanding of ASL-polynya relationships. The influence of ASL location on coastal polynya variability has not been analyzed in previous studies.

https://doi.org/10.5194/egusphere-2026-1811
Preprint. Discussion started: 4 June 2026

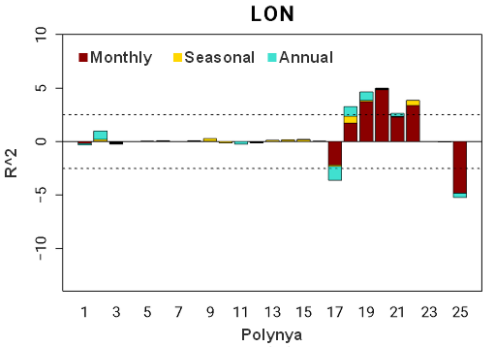

Figure 9: Coefficient of determination (R^2) of multivariate regression model results for each of the 25 Antarctic coastal polynyas regressed against the Amundsen Sea Low's longitude (LON). Red, gold, and turquoise represent relative contributions at the exclusive monthly, seasonal, and annual scales of variability, respectively. Dashed lines indicate statistical significance at the 90% level. The data ranges from April-October, 1992-2017.

Relationships between coastal polynyas and the longitudinal location of the ASL (LON) are particularly strong throughout much of West Antarctica. Statistically significant positive relationships exist in the Bellingshausen and eastern Amundsen Seas, while statistically significant negative relationships exist in the Weddell and eastern Ross Seas - all of which are driven by co-variability at the exclusive monthly temporal scale (Fig. 9). The longitudinal location of the ASL (LON) dictates the location of the meridional flow associated with the ASL, which subsequently affects polynya size.

During the study period, the ASL migrated between approximately 180-290ºE longitude. A westward (eastward) shift in LON promotes northerly (southerly) near surface wind anomalies in the Amundsen and Bellingshausen Seas [Raphael et al., 2019], significantly contributing to the closing (opening) of polynyas in that region. LON has an opposite effect in the Weddell Sea. When centered in the Amundsen-Bellingshausen region, the northerly flow on the eastern flank of the ASL reduces southerly airflow along the Ronne Ice Shelf. Also, while centered in the Amundsen-Bellingshausen region, ASL's influence on Ross Sea winds is relatively weak [Coggins and McDonald, 2015]. However, as the ASL migrates westward, southerly flow on its western flank increases polynya growth in the western Ross Sea. During the study period, the ASL seldom traveled west of 210ºE, into the Ross Sea embayment, maintaining the direct negative relationship between LON and the Okuma Bay Polynya (#25, Fig. 2a).

LON exerts a weak influence on wind variability along most of the Ross Ice Shelf during the sea ice advance season. It only influences the meridional wind at the eastern edge of the ice shelf [Raphael et al., 2019; Hosking et al., 2013], explaining its weak connection to polynyas in the western Ross Sea. LON has a statistically significant negative correlation with westerly surface wind along the Bellingshausen Sea coast [Raphael et al., 2019]. However, the relatively weak westerly wind associated with an eastward ASL position does not lead to increased polynya size, even though coastal polynya growth along the Bellingshausen coast is greatest with southeasterly wind [Nihashi and Ohshima, 2015].

https://doi.org/10.5194/egusphere-2026-1811
Preprint. Discussion started: 4 June 2026

3.6 Amundsen Sea Low: Latitude

The relationship between coastal polynya size and the Amundsen Sea Low's latitudinal position (LAT) is particularly strong in two regions - the Amundsen-Ross region in West Antarctica (#19-25) and the region spanning from Adelie Land to the Shackleton Ice Shelf in East Antarctica (#3-9). Northern (southern) ASL positions are associated with enhanced (stunted) polynya growth, particularly at the monthly and seasonal scales (Fig. 10). The ASL's importance to coastal polynya size variability is found in its effect on surface wind conditions. Sea ice motion along the Amundsen Sea coast is predominantly easterly, as it contributes to and is circulated by the Ross Gyre (Fig. 2b). Thus, the primary direction of sea ice motion during polynya expansion is easterly.

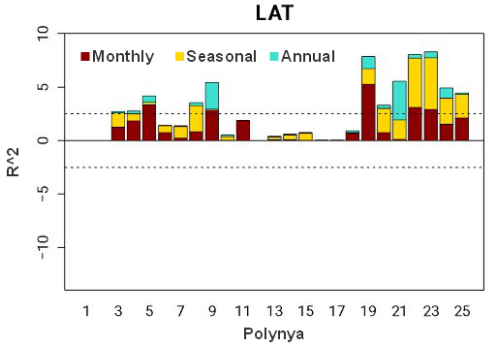

Figure 10: Coefficient of determination (R2) of multivariate regression model results for each of the 25 Antarctic coastal polynyas regressed against the Amundsen Sea Low's latitude (LAT). Red, gold, and turquoise represent relative contributions at the exclusive monthly, seasonal, and annual scales of variability, respectively. Dashed lines indicate statistical significance at the 90% level. The data ranges from April-October, 1992-2017.

Cyclonic flow around the ASL leads to easterly airflow on its southern flank, and westerly airflow on its northern flank [Raphael et al., 2019]. During the study period, the ASL migrated between approximately 62-78°S latitude. With an approximate mean ASL center location of 70°S, the geography of its easterly flow is generally aligned with mean ice motion in this region. However, during its southern migration, the ASL's easterly airflow shifts to lie over the continent and the coastal Amundsen region is influenced by the westerly airflow north of the ASL's center [Raphael et al., 2019]. This reduces easterly surface airflow, sea ice motion, and polynya expansion.

The circumAntarctic correlations between LAT and coastal polynyas are also influenced by the confounding SAM-LAT relationship. Given that East Antarctica is located outside of the ASL's domain, the positive correlations between LAT and East Antarctica polynya size are not due to a direct physical connection. Instead, they are most likely created by the SAM-LAT relationship (r=-0.29; Fig. 8), in which a northward shift in the ASL is associated with a more -SAM. Since the SAM-LAT relationship is negative, the negative SAM-polynya relationships in the Adelie-Wilkes-Shackleton region (#3-9, Fig. 2a) produce strong positive LAT-polynya correlations. Removing the influence of the SAM on ASL's latitude, would most likely result in a circumAntarctic coastal polynya correlation pattern that more closely resembles that of the ASL's longitude (LON) and relative central pressure (RCP), with all significant correlations concentrated in the ASL's West Antarctica domain - particularly spanning the Amundsen-eastern Ross region (#19-25, Fig. 2a). The absence of a statistically significant ENSO-LAT relationship (r=0.10, Fig. 8) suggests that the West Antarctic LAT-polynya relationships are not driven by a confounding influence of ENSO.

https://doi.org/10.5194/egusphere-2026-1811
Preprint. Discussion started: 4 June 2026

4. Discussion and Summary

This study uses a time series decomposition method and a circum-Antarctic coastal polynya area dataset to investigate the role that three large-scale atmospheric circulation modes - the Southern Annular Mode (SAM), El Niño-Southern Oscillation (ENSO), and the Amundsen Sea Low (ASL) - play in influencing the size of Antarctic coastal polynyas at exclusive monthly, seasonal, and annual timescales. Twenty of the twenty-five polynyas analyzed in this study are significantly influenced by at least one of the three atmospheric circulations. Three of the remaining polynyas, one in Prydz Bay and two in the Haakon VII Sea, are not significantly influenced by any of the atmospheric patterns. The final two polynyas, located in East Antarctica, are significantly correlated with the ASL. However, given how remote they are from the ASL domain, their statistical relationships are likely moderated by the SAM.

Large-scale atmospheric patterns are distinguishable features that possess distinct sizes, locations, and temporal scales of variability. The location of significant polynya-atmosphere relationships is consistent with the location of significant sea ice response to each atmospheric circulation. For example, the SAM is a circum-Antarctic phenomenon with its strongest influence on coastal sea ice occurring in East Antarctica [Raphael and Hobbs, 2014; Simpkins et al., 2012]. ENSO is a tropical phenomenon with strong global connections, and its strongest extratropical connection being the Antarctic Dipole in West Antarctica [Yuan, 2004; Liu et al., 2002]. The ASL is an exclusively West Antarctica phenomenon [Raphael et al., 2019; Hosking et al., 2013].

Coastal polynya size variability is an important function of the processes contributing to primary productivity, sea ice production, deep water formation, and the Thermohaline Circulation [Yang et al., 2025; Mizuta et al., 2024; Tamura et al., 2016; Kitade et al., 2014; Shadwick et al., 2013; Fiedler et al., 2010; Ushio et al. 1999; Beckmann et al., 1999; Smith et al., 1990]. Coastal polynyas generate approximately 10% of total Antarctic sea ice and up to 50% of ice produced in the Ross Sea [Tamura et al., 2008; Kwok et al., 2007]. With such a large proportion of Southern Ocean ice deriving from coastal polynyas, changes in polynya size affect the overall Southern Ocean ice field and the deep water generated during ice production. Since larger coastal polynyas provide more area over which processes can occur, the processes that cause coastal polynya expansion contribute to greater cumulative amounts of phytoplankton, sea ice, and deep water formation. Processes that restrict the expansion of coastal polynyas also restrict the phytoplankton, sea ice, and deep water formation.

Building on past studies that found connections between large-scale atmospheric circulation phenomena and other climate components, such as high salinity shelf water and Antarctic Bottom Water formation, we focus on the intermediary role that Antarctic coastal polynyas play in some of those processes. The atmospheric circulations' influence on coastal polynya size results from their influence on surface winds and oceanic currents. Each coastal polynya expands in specific directions that align with the flow of surface winds and ocean currents away from virtually static objects [Nihashi and Ohshima, 2015; Shadwick et al., 2013; Massom et al., 1998]. The large-scale atmospheric circulation can enhance, diminish, and redirect surface winds that flow over the coastline [Raphael et al., 2019; Coggins and McDonald, 2015; Raphael and Hobbs, 2014; Hosking et al., 2013; Turner et al., 2013; Fogt et

https://doi.org/10.5194/egusphere-2026-1811
Preprint. Discussion started: 4 June 2026

al., 2012; Turner et al., 2009; Stammerjohn et al., 2008; Yuan, 2004]. As the atmospheric circulations experience changes in their intensity and location, their impacts on surface wind and ocean currents are propagated to coastal polynyas.

We show that East Antarctic coastal polynya size variability is most influenced by the SAM at all timescales, while West Antarctic coastal polynya size variability is most influenced by ENSO and the ASL at the annual and monthly timescales, respectively. The ASL's influence is complicated by its variable intensity and location. Strong polynya responses to the ASL's actual central pressure (ACP) and location (i.e latitude) each occur at the monthly and seasonal scales. Strong polynya responses to the ASL's relative central pressure (RCP) and longitude occur primarily at the seasonal and monthly scales, respectively. These findings help to contextualize artifacts such as the strong ASL-polynya relationships in East Antarctica and the strong monthly SAM-polynya relationships hidden in previous studies conducted at the annual scale.

Polynyas along the Ross, Ronne, and Amery Ice Shelves are the greatest contributors to Antarctic Bottom Water (AABW) because of their cool, salty surface ocean layer. Other relatively prominent coastal polynyas, such as the Amundsen Sea and Bellingshausen Sea Polynyas, make smaller contributions to AABW because the ice shelves along the Amundsen and Bellingshausen Sea coasts add fresh melt water to the surface layer, increasing water buoyancy and decreasing the rate of surface waters sinking to lower depths [Silvano et al., 2018]. Since the ASL and ENSO are dominant influencers of environmental variability in the Ross and Weddell Seas, they are expected to be linked to AABW formation as well. We found that while the ASL's strength and location influences coastal polynya size in the Ross and Weddell regions, their relationships with ENSO is weak. Thus, our results suggest that the ASL may play a larger role in the variability of AABW formation than ENSO.

Future studies may further improve our general understanding of the relationships between Antarctic coastal polynyas and large-scale atmospheric patterns by analyzing polynya relationships to other climate patterns. While the SAM, ENSO, and ASL are considered great sources of Southern Ocean sea ice and wind variability, influences from other phenomena, such as the Zonal Wave 3 pattern, Pacific Decadal Oscillation, and Semi-Annual Oscillation, may also be explored. For future studies with multidecadal polynya data sets, the Pacific Decadal Oscillation, Interdecadal Pacific Oscillation, and Atlantic Multi-decadal Oscillation are good candidates for analysis. Also, the drastic change in sea ice variability beginning in 2016 highlights shifts in oceanic and atmospheric influence on the sea ice field. Future studies focused on oceanic, atmospheric, and sea ice influences on coastal polynya variability would provide great insight into the implications of the new Southern Ocean conditions, and related processes, on polynya activity.

https://doi.org/10.5194/egusphere-2026-1811
Preprint. Discussion started: 4 June 2026

Data availability

The 25-polynya dataset is accessible through the Github data repository: https://github.com/JWard31/atmos_poly/blob/e325cc43753bc6f2129a79bda6b575348879f7b5/Ward%20and%20Raphael%20-%20ACP25%20-%2025%20Antarctic%20Coastal%20Polynyas%201992-2017.csv.

The Southern Annular Mode index, described by Marshall [2003], is housed at the British Antarctic Survey (BAS; https://legacy.bas.ac.uk/met/gjma/sam.html).

The Southern Oscillation Index (SOI) used to characterize the ENSO pattern is distributed by the National Oceanic and Atmospheric Administration (https://www.cpc.ncep.noaa.gov/data/indices/soi).

The Amundsen Sea Low dataset is also distributed by BAS, and it was created using the method described by Hosking et al. [2013; https://scotthosking.com/asl_index].

Author contributions

JW conceptualized original research goals, created the polynya dataset, retrieved additional data sets, conducted statistical analyses and other investigative processes, interpreted results, prepared figures, and wrote the initial draft. MR advised on overarching concepts and research plans, interpreted results, edited the paper, and provided the funding used during the project.

Financial support

This research was supported by the National Science Foundation, Office of Polar Programs (grant no. NSF-OPP-1745089).

https://doi.org/10.5194/egusphere-2026-1811
Preprint. Discussion started: 4 June 2026

References

Ackley, S. F., Geiger, C. A., King, J. C., Hunke, E. C., & Comiso, J. (2001). The Ronne polynya of 1997/98: observations of air-ice-ocean interaction. Annals of Glaciology, 33, 425-429. https://doi.org/10.3189/172756401781818725

Adolphs, U., & Wendler, G. (1995). A pilot study on the interactions between katabatic winds and polynyas at the Adélie Coast, eastern Antarctica. Antarctic Science, 7(3), 307-314. https://doi.org/10.1017/S0954102095000423

Arblaster, J. M., & Meehl, G. A. (2006). Contributions of external forcings to southern annular mode trends [Article]. Journal of Climate, 19(12), 2896-2905. https://doi.org/10.1175/jcli3774.1

Armstrong, R., K. Knowles, M. J. Brodzik, and M. A. Hardman (1994), DMSP SSM/I-SSMIS Pathfinder Daily EASE-Grid Brightness Temperatures, Version 2. Used subset with years 1992-2017. Boulder, Colorado USA. NASA National Snow and Ice Data Center Distributed Active Archive Center. doi: https://doi.org/10.5067/3EX2U1DV3434. Accessed October 1, 2017.

Arrigo, K. R., & van Dijken, G. L. (2003). Phytoplankton dynamics within 37 Antarctic coastal polynya systems. Journal of Geophysical Research-Oceans, 108(C8), Article 3271. https://doi.org/10.1029/2002jc001739

Arrigo, K. R., & van Dijken, G. L. (2004). Annual changes in sea-ice, chlorophyll a, and primary production in the Ross Sea, Antarctica. Deep-Sea Research Part Ii-Topical Studies in Oceanography, 51(1-3), 117-138. https://doi.org/10.1016/j.dsr2.2003.04.003

Beckmann, A., Hellmer, H. H., & Timmermann, R. (1999). A numerical model of the Weddell Sea: Large-scale circulation and water mass distribution. Journal of Geophysical Research-Oceans, 104(C10), 23375-23391. https://doi.org/10.1029/1999jc900194

Bromwich D.H., A.J. Monaghan, A.N. Rogers, M.L. Van Woert, K.R. Arrigo (1998), Winter Atmospheric Forcing of the Ross Sea Polynya, American Geophysical Union – Ocean, Ice, And Atmosphere: Interactions At The Antarctic Continental Margin, Antarctic Research Series, 75, 101-133, http://citeseerx.ist.psu.edu/viewdoc/download?doi=10.1.1.515.5490&rep=rep1&type=pdf

Campbell, E., Wilson, E., Moore, G., Riser, S., Brayton, C., Mazloff, M., & Talley, L. (2019). Antarctic offshore polynyas linked to Southern Hemisphere climate anomalies [Article]. NATURE, 570(7761), 319-+. https://doi.org/10.1038/s41586-019-1294-0

Cheon, W., & Gordon, A. (2019). Open-ocean polynyas and deep convection in the Southern Ocean [Article]. SCIENTIFIC REPORTS, 9, Article 6935. https://doi.org/10.1038/s41598-019-43466-2

Coggins, J. H. J., & McDonald, A. J. (2015). The influence of the Amundsen Sea Low on the winds in the Ross Sea and surroundings: Insights from a synoptic climatology. Journal of Geophysical Research-Atmospheres, 120(6), 2167-2189. https://doi.org/10.1002/2014jd022830

Comiso, J. C., Kwok, R., Martin, S., & Gordon, A. L. (2011). Variability and trends in sea ice extent and ice production in the Ross Sea. Journal of Geophysical Research-Oceans, 116, Article C04021. https://doi.org/10.1029/2010jc006391

https://doi.org/10.5194/egusphere-2026-1811
Preprint. Discussion started: 4 June 2026

Drucker, R., Martin, S., & Kwok, R. (2011). Sea ice production and export from coastal polynyas in the Weddell and Ross Seas. Geophysical Research Letters, 38, Article L17502. https://doi.org/10.1029/2011gl048668

Faraway, J. J., (2014). Linear Models with R. 2nd Edition. Chapman and Hall. https://doi.org/10.1201/b17144

Fiedler, E. K., Lachlan-Cope, T. A., Renfrew, I. A., & King, J. C. (2010). Convective heat transfer over thin ice covered coastal polynyas. Journal of Geophysical Research-Oceans, 115, Article C10051. https://doi.org/10.1029/2009jc005797

Fogt, R. L., Wovrosh, A. J., Langen, R. A., & Simmonds, I. (2012). The characteristic variability and connection to the underlying synoptic activity of the Amundsen-Bellingshausen Seas Low. Journal of Geophysical Research-Atmospheres, 117, Article D07111. https://doi.org/10.1029/2011jd017337

Gillett, N. P., Stone, D. A., Stott, P. A., Nozawa, T., Karpechko, A. Y., Hegerl, G. C.,…Jones, P. D. (2008). Attribution of polar warming to human influence. Nature Geoscience, 1(11), 750-754. https://doi.org/10.1038/ngeo338

Goosse, H., & Fichefet, T. (2001). Open-ocean convection and polynya formation in a large-scale ice-ocean model. Tellus A, 53(1), 94-111. https://doi.org/10.1034/j.1600-0870.2001.01061.x

Holland, P. R., & Kwok, R. (2012). Wind-driven trends in Antarctic sea-ice drift. Nature Geoscience, 5(12), 872-875. https://doi.org/10.1038/ngeo1627

Hosking, J. S., Orr, A., Marshall, G. J., Turner, J., & Phillips, T. (2013). The Influence of the Amundsen-Bellingshausen Seas Low on the Climate of West Antarctica and Its Representation in Coupled Climate Model Simulations. Journal of Climate, 26(17), 6633-6648. https://doi.org/10.1175/jcli-d-12-00813.1

Jiang, N., Zhang, Z., Zhang, R., Wang, C., & Zhou, M. (2024). The connection of phytoplankton biomass in the Marguerite Bay polynya of the western Antarctic Peninsula to the Southern Annular Mode [Article]. ACTA OCEANOLOGICA SINICA, 43(1), 35-47. https://doi.org/10.1007/s13131-023-2201-y

Kitade, Y., Shimada, K., Tamura, T., Williams, G. D., Aoki, S., Fukamachi, Y.,…Ohshima, K. I. (2014). Antarctic Bottom Water production from the Vincennes Bay Polynya, East Antarctica. Geophysical Research Letters, 41(10), 3528-3534. https://doi.org/10.1002/2014gl059971

Knuth, S. L., & Cassano, J. J. (2011). An Analysis of Near-Surface Winds, Air Temperature, and Cyclone Activity in Terra Nova Bay, Antarctica, from 1993 to 2009. Journal of Applied Meteorology and Climatology, 50(3), 662-680. https://doi.org/10.1175/2010jamc2507.1

Kwok, R., Comiso, J. C., Martin, S., & Drucker, R. (2007). Ross Sea polynyas: Response of ice concentration retrievals to large areas of thin ice. Journal of Geophysical Research-Oceans, 112(C12), Article C12012. https://doi.org/10.1029/2006jc003967

Liu, J., Yuan, X., Rind, D., & Martinson, D. G. (2002). Mechanism study of the ENSO and southern high latitude climate teleconnections. Geophysical Research Letters, 29(14), 24-1. https://doi.org/10.1029/2002GL015143

Maksym, T., Stammerjohn, S. E., Ackley, S., & Massom, R. (2012). Antarctic Sea Ice-A Polar Opposite? Oceanography, 25(3), 140-151. https://www.jstor.org/stable/24861407

https://doi.org/10.5194/egusphere-2026-1811
Preprint. Discussion started: 4 June 2026

737 Marshall, G. J. (2003). Trends in the southern annular mode from observations and reanalyses. Journal of Climate,
738 16(24), 4134-4143. https://doi.org/10.1175/1520-0442(2003)016<4134:titsam>2.0.co;2
739 Martin, S., Drucker, R. S., & Kwok, R. (2007). The areas and ice production of the western and central Ross Sea
740 polynyas, 1992-2002, and their relation to the B-15 and C-19 iceberg events of 2000 and 2002. Journal of Marine
741 Systems, 68(1-2), 201-214. https://doi.org/10.1016/j.jmarsys.2006.11.008
742 Massom, R. A., Harris, P. T., Michael, K. J., & Potter, M. J. (1998). The distribution and formative processes of
743 latent-heat polynyas in East Antarctica. Annals of Glaciology, 27, 420-426.
744 https://doi.org/10.3189/1998AoG27-1-420-426
745 Mizuta, G., Ohshima, K., Takatsuka, T., Kitade, Y., Fujii, M., Nakayama, Y., & Ikehara, M. (2024). Circulation and
746 production of Cape Darnley Bottom Water on the continental slope off the Cape Darnley polynya, East Antarctica
747 [Article]. DEEP-SEA RESEARCH PART I-OCEANOGRAPHIC RESEARCH PAPERS, 211, Article 104362.
748 https://doi.org/10.1016/j.dsr.2024.104362
749 Montes-Hugo, M. A., & Yuan, X. (2012). Climate patterns and phytoplankton dynamics in Antarctic latent heat
750 polynyas. Journal of Geophysical Research-Oceans, 117, Article C05031. https://doi.org/10.1029/2010jc006597
751 National Oceanic and Atmospheric Administration, Southern Oscillation Index, Climate Prediction Center,
752 https://www.cpc.ncep.noaa.gov/data/indices/soi
753 Nicholls, K.W. (2001), Sub Ice-Shelf Circulation and Processes, Ocean Currents, Elsevier Ltd. – 1st edition of
754 Encyclopedia of Ocean Sciences, 5, 2892–2901, Book.
755 Nicholls, N. (2008). Recent trends in the seasonal and temporal behaviour of the El Nino-Southern Oscillation
756 [Article]. Geophysical Research Letters, 35(19), 4, Article L19703. https://doi.org/10.1029/2008gl034499
757 Nihashi, S., & Ohshima, K. I. (2015). Circumpolar Mapping of Antarctic Coastal Polynyas and Landfast Sea Ice:
758 Relationship and Variability. Journal of Climate, 28(9), 3650-3670. https://doi.org/10.1175/jcli-d-14-00369.1
759 Nihashi, S., Ohshima, K. I., & Tamura, T. (2017). Sea-Ice Production in Antarctic Coastal Polynyas Estimated From
760 AMSR2 Data and Its Validation Using AMSR-E and SSM/I-SSMIS Data. Ieee Journal of Selected Topics in
761 Applied Earth Observations and Remote Sensing, 10(9), 3912-3922. https://doi.org/10.1109/jstars.2017.2731995
762 Ohshima, K., Nihashi, S., & Iwamoto, K. (2016). Global view of sea-ice production in polynyas and its linkage to
763 dense/bottom water formation [Review]. GEOSCIENCE LETTERS, 3, Article 13.
764 https://doi.org/10.1186/s40562-016-0045-4
765 Park, J., Kim, H. C., Jo, Y. H., Kidwell, A., & Hwang, J. (2018). Multi-temporal variation of the Ross Sea Polynya
766 in response to climate forcings. Polar Research, 37, 13, Article 1444891.
767 https://doi.org/10.1080/17518369.2018.1444891
768 Raphael, M., & Hobbs, W. (2014). The influence of the large-scale atmospheric circulation on Antarctic sea ice
769 during ice advance and retreat seasons. GEOPHYSICAL RESEARCH LETTERS, 41(14), 5037-5045.
770 https://doi.org/10.1002/2014GL060365

https://doi.org/10.5194/egusphere-2026-1811
Preprint. Discussion started: 4 June 2026

Raphael, M., Holland, M., Landrum, L., & Hobbs, W. (2019). Links between the Amundsen Sea Low and sea ice in the Ross Sea: seasonal and interannual relationships. CLIMATE DYNAMICS, 52(3-4), 2333-2349. https://doi.org/10.1007/s00382-018-4258-4

Shadwick, E. H., Rintoul, S. R., Tilbrook, B., Williams, G. D., Young, N., Fraser, A. D., Marchant, H., Smith, J., & Tamura, T. (2013). Glacier tongue calving reduced dense water formation and enhanced carbon uptake. Geophysical Research Letters, 40(5), 904-909. https://doi.org/10.1002/grl.50178

Silvano, A., Narayanan, A., Catany, R., Olmedo, E., González-Gambau, V., Turiel, R. Sabia, M.R. Mazloff, T. Spira, F.A. Haumann, & A.C. Naveira Garabato, A. C. (2025). Rising surface salinity and declining sea ice: A new Southern Ocean state revealed by satellites. Proceedings of the National Academy of Sciences, 122(27), e2500440122. https://doi.org/10.1073/pnas.2500440122

Silvano, A., Rintoul, S.R., Peña-Molino, B., Hobbs, W.R., van Wijk, E., Aoki, S., Tamura, T. and Williams, G.D. (2018). Freshening by glacial meltwater enhances melting of ice shelves and reduces formation of Antarctic Bottom Water. Science advances, 4(4), eaap9467. https://doi.org/10.1126/sciadv.aap9467

Simpkins, G. R., Ciasto, L. M., Thompson, D. W. J., & England, M. H. (2012). Seasonal Relationships between Large-Scale Climate Variability and Antarctic Sea Ice Concentration. Journal of Climate, 25(16), 5451-5469. https://doi.org/10.1175/jcli-d-11-00367.1

Smith, S. D., Muench, R. D., & Pease, C. H. (1990). Polynyas and leads: An overview of physical processes and environment. Journal of Geophysical Research: Oceans, 95(C6), 9461-9479. https://doi.org/10.1029/JC095iC06p09461

Stammerjohn, S. E., Martinson, D. G., Smith, R. C., Yuan, X., & Rind, D. (2008), Trends in Antarctic annual sea ice retreat and advance and their relation to El Niño–Southern Oscillation and Southern Annular Mode variability, J. Geophys. Res., 113, C03S90, https://doi.org/10.1029/2007JC004269

Tamura, T., Ohshima, K. I., Fraser, A. D., & Williams, G. D. (2016). Sea ice production variability in Antarctic coastal polynyas. Journal of Geophysical Research-Oceans, 121(5), 2967-2979. https://doi.org/10.1002/2015jc011537

Tamura, T., Ohshima, K. I., Markus, T., Cavalieri, D. J., Nihashi, S., & Hirasawa, N. (2007). Estimation of thin ice thickness and detection of fast ice from SSM/I data in the Antarctic Ocean. Journal of Atmospheric and Oceanic Technology, 24(10), 1757-1772. https://doi.org/10.1175/jtech2113.1

Tamura, T., Ohshima, K. I., & Nihashi, S. (2008). Mapping of sea ice production for Antarctic coastal polynyas. Geophysical Research Letters, 35(7), Article L07606. https://doi.org/10.1029/2007gl032903

Thompson, D. W. J., Solomon, S., Kushner, P. J., England, M. H., Grise, K. M., & Karoly, D. J. (2011). Signatures of the Antarctic ozone hole in Southern Hemisphere surface climate change [Review]. Nature Geoscience, 4(11), 741-749. https://doi.org/10.1038/ngeo1296

Tschudi, M., C. Fowler, J. Maslanik, J. S. Stewart, and W. N. Meier. 2016. Polar Pathfinder Daily 25 km EASE-Grid Sea Ice Motion Vectors, Version 3. April-October, 1992-2016. Boulder, Colorado USA. NASA National Snow and Ice Data Center Distributed Active Archive Center. https://doi.org/10.5067/O57VAIT2AYYY

https://doi.org/10.5194/egusphere-2026-1811
Preprint. Discussion started: 4 June 2026

807 Turner, J., Comiso, J. C., Marshall, G. J., Lachlan-Cope, T. A., Bracegirdle, T., Maksym, T.,…Orr, A. (2009).
808 Non-annular atmospheric circulation change induced by stratospheric ozone depletion and its role in the recent
809 increase of Antarctic sea ice extent. Geophysical Research Letters, 36, Article L08502.
810 https://doi.org/10.1029/2009gl037524
811 Turner, J., Hosking, J. S., Marshall, G. J., Phillips, T., & Bracegirdle, T. J. (2016). Antarctic sea ice increase
812 consistent with intrinsic variability of the Amundsen Sea Low. Climate Dynamics, 46(7-8), 2391-2402.
813 https://doi.org/10.1007/s00382-015-2708-9
814 Turner, J., Phillips, T., Hosking, J. S., Marshall, G. J., & Orr, A. (2013). The Amundsen Sea Low. International
815 Journal of Climatology, 33(7), 1818-1829. https://doi.org/10.1002/joc.3558
816 Ushio, S., Takizawa, T., Ohshima, K. I., & Kawamura, T. (1999). Ice production and deep-water entrainment in shelf
817 break polynya off Enderby Land, Antarctica. Journal of Geophysical Research-Oceans, 104(C12), 29771-29780.
818 https://doi.org/10.1029/1999jc900249
819 Ward, J. and Raphael, M. (2018). ACP25 - 25 Antarctic Coastal Polynyas 1992-2017.csv., Github,
820 https://github.com/JWard31/atmos_poly/blob/e325cc43753bc6f2129a79bda6b575348879f7b5/Ward%20and%20Ra
821 phael%20-%20ACP25%20-%2025%20Antarctic%20Coastal%20Polynyas%201992-2017.csv
822 Ward, J. (2018). Multi-Temporal Variability Within Antarctic Coastal Polynyas and Their Relationships To
823 Large-Scale Atmospheric Phenomena. UCLA. ProQuest ID: Ward_ucla_0031D_17468. Merritt ID:
824 ark:/13030/m5gx98s2. Retrieved from https://escholarship.org/uc/item/0tj68195
825 Yang, K., Wu, J., Li, H., Xu, F., & Zhang, M. (2025). Map of Arctic and Antarctic Polynyas 2013-2022 Using Sea
826 Ice Concentration [Article]. REMOTE SENSING, 17(7), Article 1213. https://doi.org/10.3390/rs17071213
827 Yuan, X. J. (2004). ENSO-related impacts on Antarctic sea ice: a synthesis of phenomenon and mechanisms.
828 Antarctic Science, 16(4), 415-425. https://doi.org/10.1017/s0954102004002238
829 Yuan, X. J., & Martinson, D. G. (2001). The Antarctic Dipole and its predictability. Geophysical Research Letters,
830 28(18), 3609-3612. https://doi.org/10.1029/2001gl012969
831 Zwally, H. J., Comiso, J. C., & Gordon, A. L. (1985). Antarctic offshore leads and polynyas and oceanographic
832 effects. Oceanology of the Antarctic continental shelf, 43, 203-226.
833 https://agupubs.onlinelibrary.wiley.com/doi/10.1029/AR043p0203
834